

Leveraging Joint Predictive Embedding and Bayesian Inference in Graph Self Supervised Learning

Srinitish Srinivasan

*School of Computer Science and Engineering
Vellore Institute of Technology*

srinitish.srinivasan2021@vitstudent.ac.in

Omkumar CU

*School of Computer Science and Engineering
Vellore Institute of Technology*

omkumar.cu@vit.ac.in

Abstract

Graph representation learning has emerged as a cornerstone for tasks like node classification and link prediction, yet prevailing self-supervised learning (SSL) methods face challenges such as computational inefficiency, reliance on contrastive objectives, and representation collapse. Existing approaches often depend on feature reconstruction, negative sampling, or complex decoders, which introduce training overhead and hinder generalization. Further, current techniques which address such limitations fail to account for the contribution of node embeddings to a certain prediction in the absence of labeled nodes. To address these limitations, we propose a novel joint embedding predictive framework for graph SSL that eliminates contrastive objectives and negative sampling while preserving semantic and structural information. Additionally, we introduce a semantic-aware objective term that incorporates pseudo-labels derived from Gaussian Mixture Models (GMMs), enhancing node discriminability by evaluating latent feature contributions. Extensive experiments demonstrate that our framework outperforms state-of-the-art graph SSL methods across benchmarks, achieving superior performance without contrastive loss or complex decoders. Key innovations include (1) a non-contrastive, view-invariant joint embedding predictive architecture, (2) leveraging single context and multiple targets relationship between subgraphs, and (3) GMM-based pseudo-label scoring to capture semantic contributions. This work advances graph SSL by offering a computationally efficient, collapse-resistant paradigm that bridges spatial and semantic graph features for downstream tasks. The code for our paper can be found at <https://github.com/Deceptrax123/JPEB-GSSL>.

1 Introduction

Graph representation learning has found widespread adoption in Social Network Analysis, Recommendation Systems, Computer Vision and Natural Language Processing Wu et al. (2020). It aims to learn low-dimensional embeddings of nodes or subgraphs while preserving their underlying spatial and spectral features. These learned embeddings can then be used on downstream tasks such as node classification (Maekawa et al., 2022), link prediction (Zhang & Chen, 2018) and community detection (Li et al., 2024) by training task-specific decoders or classification layers on the learned embeddings keeping the backbone frozen. Such an approach reduces the computational complexity and training time on downstream tasks. Though Graph Neural Networks (GNNs) have gained popularity over time, they require a certain number of labelled nodes to perform well. Further, owing to the complexity of graph representations spatially, it is often challenging to pre-train graphs and transfer the learned embeddings to downstream tasks.

Graph Self Supervised learning has been widely studied in the literature to facilitate graph representation learning. This includes methods such as Node2Vec, DGI (Veličković et al., 2018), MVGRL (Hassani & Khasahmadi, 2020), GRACE (Zhu et al., 2020) etc. Although these methods have achieved state-of-the-art

results on several social networks, they rely heavily on either graph reconstruction/feature reconstruction, re-masking or generating contrastive views by negative sampling, which is a computationally expensive process on large graphs. Graph-SSL methods that rely on reconstruction (generative methods) are decoder variant, meaning they depend on the decoder architecture(inner product decoder or symmetrical feature reconstruction). Such networks might require additional feature propagation steps such as skip connections to prevent vanishing gradients and retain learned information. Furthermore, most methods tend to use more layers or stack multiple encoders to capture long-range node interactions, which increases training complexity and leads to poor performance in downstream tasks due to over-smoothing. This diminishes the model’s ability to effectively discriminate between nodes effectively(Wang et al., 2024).

To address the limitations of existing methods, we introduce a joint embedding predictive framework that predicts subgraph embeddings of randomly sampled targets given a context conditioned on a latent variable z . The framework employs two encoders: a context encoder, which processes subgraphs sampled by randomly dropping nodes and updates its parameters dynamically through gradient descent, and a target encoder, whose weights are maintained as a moving average of the context encoder. The target encoder processes the original graph (without any view augmentations) to generate target node representations. Subsequently, three subgraphs are sampled from the latent space by randomly masking the target node representations. These sampled subgraphs are then fed into a global mean pooling operation to compute their embeddings, which serve as targets for a single context. To prevent representational collapse, we incorporate positional information of target nodes into the context embeddings before deriving subgraph views. A predictor network then maps the context embeddings with target positional information to the corresponding target embeddings. However, optimizing solely on context-target embeddings risks overlooking the graph’s semantic information. To overcome this, we enhance node representations by introducing an additional term to the objective function, scoring pseudo-labels predicted from the node embeddings. This is achieved by fitting a Gaussian Mixture Model (GMM) on the embeddings and evaluating the contribution of each latent feature to the pseudo-labels. Through this design, we present a graph augmentation and view invariant self-supervised learning technique that avoids the need for negative samples or contrastive objectives based on mutual information estimators. This offers a robust alternative for representation learning in graph-based applications.

We list our main contributions as follows:

- We introduce a novel graph self supervised learning method based on a joint predictive embedding paradigm which bypasses contrastive objectives such as Mutual Information(MI) Estimators, contrastive example generation techniques such as negative sampling and avoids noisy features.
- Through our technique, we account for representation collapse by sampling multiple target embeddings for a single context, thereby enhancing the spread of node representations, and by providing positional information of target nodes to the context subgraph.
- We also account for contribution of node embeddings to pseudo-label level predictions by incorporating an additional term to the joint predictive objective. This is given by scoring pseudo-labels generated by fitting a Gaussian Mixture Model(GMM) on the learned node embeddings.
- We conduct extensive experiments demonstrating that our approach significantly outperforms previous state-of-the-art Graph Self-Supervised Learning (G-SSL) methods. Additionally, we provide a thorough empirical efficiency analysis highlighting the model’s efficiency and scalability.

2 Related Work

2.1 Unsupervised Representation Learning on Graphs

(Jin et al., 2021b) proposes a method for composing multiple self-supervised tasks for GNNs. They introduce a pseudo-homophily measure to evaluate representation quality without labels. (Zhang et al., 2021) proposed the removal of negative sampling and MI estimator optimization entirely. The authors propose a loss function that contains an invariance term that maximizes correlation between embeddings of the two views and a

decorrelation term that pushes different feature dimensions to be uncorrelated. (Hou et al., 2022) employs a re-mask decoding strategy and uses expressive GNN decoders instead of Multi-Layer Perceptrons (MLPs) enabling the model to learn more meaningful compressed representations. It lays focus on masked feature reconstruction rather than structural reconstruction. (Hassani & Khasahmadi, 2020) proposed MVGRL that makes use of two graph views and a discriminator to maximize mutual information between node embeddings from a first-order view and graph embeddings from a second-order view. It leverages both node and graph-level embeddings and avoids the need for explicit negative sampling. (Ju et al., 2022) proposed ParetoGNN which simultaneously learns from multiple pretext tasks spanning different philosophies. It uses a multiple gradient descent algorithm to dynamically reconcile conflicting learning objectives, showing state-of-the-art performance in node classification, clustering, link prediction and community prediction.

2.2 Bootstrapping Methods

(Ding et al., 2023) introduced multi-scale feature propagation to capture long-range node interactions without oversmoothing. The authors also enhance inter-cluster separability and intra-cluster compactness by inferring cluster prototypes using a Bayesian non-parametric approach via Dirichlet Process Mixture Models (DPMMs). (Thakoor et al., 2021) makes use of simple graph augmentations such as random node feature and edge masking, making it easier to implement on large graphs while achieving state-of-the-art results. It leverages a cosine similarity-based objective to make the predicted target representations closer to the true representations. (Jin et al., 2021a) introduced a Siamese network architecture comprising an online and target encoder with momentum-driven update steps for the target. The authors propose 2 contrastive objectives i.e cross-network and cross view-contrastiveness. The Cross-network contrastive objective incorporates negative samples to push disparate nodes away in different graph views to effectively learn topological information.

2.3 Joint Predictive Embedding Methods

Joint predictive embedding has been explored in the field of computer vision and audio recognition. (Assran et al., 2023) introduced I-JEPA which eliminates the need for hand-crafted augmentations and image reconstruction. They make use of a joint-embedding predictive model that predicts representations of masked image regions in an abstract feature space rather than in pixel space, allowing the model to focus on high-level semantic structures. It makes use of a Vision Transformer (ViT) with a multi-block masking strategy ensuring that the predictions retain semantic integrity. (Fei et al., 2023) extends the masked-modeling principle from vision to audio, enabling self-supervised learning on spectrograms. The key technical contribution is the introduction of a curriculum masking strategy, which transitions from random block masking to time-frequency-aware masking, addressing the strong correlations in audio spectrograms.

3 Methodology

3.1 Preliminaries

Consider the definition of a Graph $G = (V, E)$. Let V be the set of vertices $\{v_1, v_2, v_3 \dots v_{n_v}\}$ and E be the set of edges $\{e_1, e_2, e_3 \dots e_{n_e}\}$. n_v, n_e are the number of nodes and edges respectively in G . Each node in V is characterized by a d dimensional vector. This is the initial signal that is populated by either bag of words or binary values depending on the problem considered.

3.2 Loss Function

3.2.1 Joint Predictive Optimization

We sample a subgraph G' from graph G by dropping a set of nodes according to a Bernoulli distribution parameterized by success probability p_1 . The subgraph G' is passed into the context encoder to output node embeddings H' of dimensions d' . Meanwhile, the graph G is passed into the target encoder to generate node embeddings H with the same dimensions as H' . At the latent space, we sample 3 target subgraphs from the

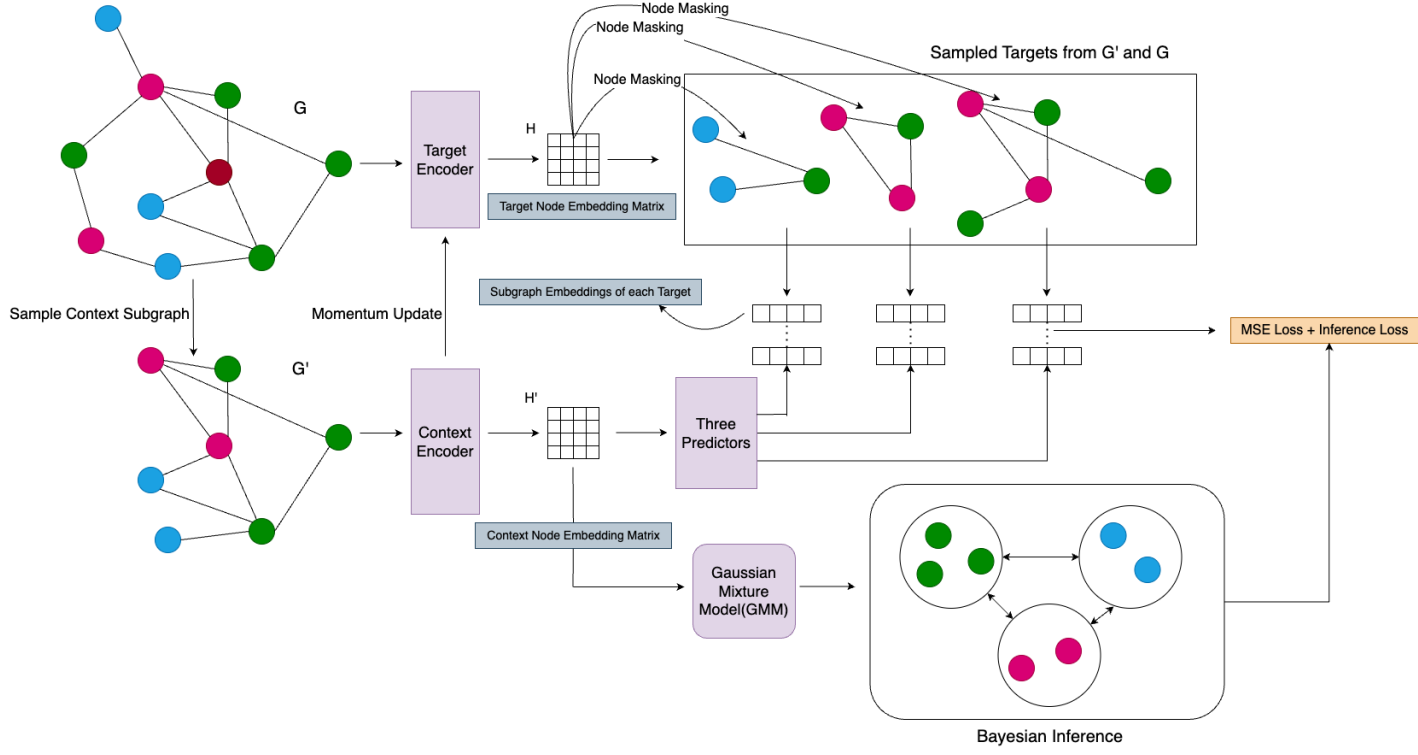


Figure 1: Overall Framework Diagram

context subgraph G' , again according to a Bernoulli distribution with probability p_2 such that $p_2 < p_1$. The node embeddings of each subgraph are obtained by deactivating the node features of masked nodes, which is followed by global mean pooling operation, thus obtaining embeddings H_1^t, H_2^t and H_3^t . The context node level embeddings H' is passed into 3 predictors, corresponding to the three target subgraphs. The obtained predictions are then pooled by the mean pooling operation, thus resulting in target predictions H'_1, H'_2, H'_3 , conditioned on latent variable H' . We then frame the objective function for the joint predictive component as follows,

$$\mathcal{L}^J(\Theta^C, \Theta^R) = \frac{1}{T} \sum_{k=1}^{k=T} \|H'_k - H_k^t\|^2 \quad (1)$$

where T is the total number of targets, Θ^C is the weight matrix of the context encoder and Θ^R is the weight matrix of the target encoder. The objective is computed at the latent space with no reconstruction/negative sampling involved.

3.2.2 Node Feature Contribution Optimization

The node embeddings H' obtained from passing G' into the context encoder are fit in a Gaussian Mixture Model(GMM). We aim to obtain,

$$p(z_k = 1 | h'_n) = \frac{p(h'_n | z_k = 1)p(z_k = 1)}{\sum_{j=1}^{j=K} p(h'_n | z_j = 1)p(z_j = 1)} \quad (2)$$

where z is a latent variable that takes 2 values: one if h' comes from Gaussian k , and zero otherwise. We can obtain,

$$p(z_k = 1) = \pi_k \quad (3)$$

$$p(h'_n | z_k = 1) = \mathcal{N}(h'_n | \mu_k, \Sigma_k) \quad (4)$$

where π_k is the mixing coefficient such that,

$$\sum_{k=1}^{k=K} \pi_k = 1 \quad (5)$$

On replacing these equations in eq.2, we obtain

$$p(z_k = 1|h'_n) = \frac{\pi_k \mathcal{N}(h'_n|\mu_k, \Sigma_k)}{\sum_j \pi_j \mathcal{N}(h'_n|\mu_j, \Sigma_j)} = \gamma(z_{nk}) \quad (6)$$

E-Step: In the E-Step, we aim to evaluate,

$$\mathcal{Q}(\theta^*, \theta) = \mathbb{E}[\ln p(H', Z|\theta^*)] = \sum_Z p(Z|H', \theta) \ln p(H', Z|\theta^*) \quad (7)$$

from eq.6, we can substitute γ in the above equation as,

$$\mathcal{Q}(\theta^*, \theta) = \sum_Z \gamma(z_{nk}) \ln p(H', Z|\theta^*) \quad (8)$$

On finding the complete likelihood of the model, we finally have,

$$\mathcal{Q}(\theta^*, \theta) = \sum_{n=1}^N \sum_{k=1}^K \gamma(z_{nk}) [\ln \pi_k + \ln \mathcal{N}(h'_n|\mu_k, \Sigma_k)] \quad (9)$$

M-Step: In the M-Step, we aim to find updated parameters θ^* as follows,

$$\theta^* = \arg \max_{\theta} \mathcal{Q}(\theta^*, \theta) \quad (10)$$

Considering the restriction, $\sum_{k=1}^K \pi_k = 1$, eq.9 is modified as follows,

$$\mathcal{Q}(\theta^*, \theta) = \sum_{n=1}^N \sum_{k=1}^K \gamma(z_{nk}) [\ln \pi_k + \ln \mathcal{N}(h'_n|\mu_k, \Sigma_k)] - \lambda (\sum_{k=1}^K \pi_k - 1) \quad (11)$$

The parameters are then determined by finding the maximum likelihood of \mathcal{Q} . On taking the derivative with respect to π_k, μ_k, Σ_k and rearranging terms, we finally obtain the update equations for the parameters as follows,

$$\pi_k = \frac{\sum_{n=1}^N \gamma(z_{nk})}{N} \quad (12)$$

$$\mu_k^* = \frac{\sum_{n=1}^N \gamma(z_{nk}) h'_n}{\sum_{n=1}^N \gamma(z_{nk})} \quad (13)$$

$$\sum_k^* = \frac{\sum_{n=1}^N \gamma(z_{nk}) (h'_n - \mu_k)(h'_n - \mu_k)^T}{\sum_{n=1}^N \gamma(z_{nk})} \quad (14)$$

Parameter Θ^C Update: Let V_g be a vector of pseudo-labels obtained for each node from the Gaussian Mixture Model(GMM) and V_k be the vector of pseudo-labels obtained by clustering node embeddings H' by K-Means. We update the context encoder parameters Θ^c with the following objective,

$$\mathcal{L}^G = \begin{cases} 0.5 \left(\frac{V_g^T H'}{\|V_g\|} - \frac{V_k^T H'}{\|V_k\|} \right) / \beta, & \text{if } \left| \frac{V_g^T H'}{\|V_g\|} - \frac{V_k^T H'}{\|V_k\|} \right| < \beta \\ \left| \frac{V_g^T H'}{\|V_g\|} - \frac{V_k^T H'}{\|V_k\|} \right| - 0.5\beta, & \text{otherwise} \end{cases} \quad (15)$$

In the above equation, the context encoder parameters Θ^c are updated by the smooth L_1 loss function.

3.2.3 Final objective

The context encoder parameters Θ^C are finally updated as follows,

$$\mathcal{L} = \mathcal{L}^J + \mathcal{L}^G \quad (16)$$

$$\Theta^C \leftarrow \text{optimize}(\Theta^c, \alpha, \partial_{\Theta^c} \mathcal{L}) \quad (17)$$

where, α is the learning rate for the Adam optimizer. The weights of the context and target encoder are randomly initialized by a standard normal distribution. A cosine annealing learning rate scheduler with early stopping is used in all experiments.

3.3 Description of Components and Operations

3.3.1 Context Encoder

The node features from G' are passed into the context encoder. The context encoder is a simple 3-layer GCN encoder which predicts 128, 256 and 512 features in each layer respectively. The forward propagation for each layer is described as follows,

$$X' = g(\hat{D}^{-\frac{1}{2}} \hat{A} \hat{D}^{-\frac{1}{2}} X \Theta) \quad (18)$$

$$\hat{A} = A + I \quad (19)$$

where \hat{D} is the degree matrix, \hat{A} is the adjacency matrix with added self-loops and Θ is the learned weights matrix. g is a non-linear function. We use ReLU for the first two layers and Tanh for the final layer. The context encoder is an online encoder whose weights are updated by gradient descent.

3.3.2 Target Encoder

The target encoder inputs node features from G . Similar to the context encoder, it is a 3-layer GCN encoder with same number of hidden, output dimensions and forward propagation steps. The weights of the target encoder are updated as a moving average of the context encoder as follows,

$$\Theta_s^R = m\Theta_{s-1}^R + (1 - m)\Theta_s^C \quad (20)$$

where Θ^R is the weights matrix of the target encoder, Θ^C is the weights of the context encoder, m is the momentum parameter and s refers to the sth iteration.

3.3.3 Predictor

The predictor consists of 2 GCN layers, both predicting 512 features. The activation function g for both layers is Tanh, in line with the final layer of the target encoder. We use Tanh since it is a bounded function, thus stabilizing the loss computation and optimization.

3.3.4 Global Mean Pooling Operation

The global mean pool operation for a graph G is given as follows,

$$r = \frac{1}{N} \sum_{n=1}^{n=N} x_n \quad (21)$$

where x_n refers to the node features of node n and N is the total number of nodes in graph G

3.4 Implementation Details

For all experiments, we use the Adam Optimizer(Kingma, 2014) and cosine annealing learning rate scheduler with warm restarts. No regularization techniques such as dropout, L_1 or L_2 have been employed since they tend to reduce performance. For learning rates, we perform a search with values corresponding to the search space $\{0.5, 0.1, 0.05, 0.01, 0.001\}$. We set the value of the momentum update parameter m to 0.9. The number of epochs was set to 50,000 with early stopping. All experiments were conducted on an M2 Macbook Pro with 8GB CPU.

4 Experiments

4.1 Experimental Setting

4.1.1 Datasets

In our experiments, we evaluate our proposed framework on seven publicly available benchmark datasets for node representation learning and classification. The datasets are, namely, Cora(Sen et al., 2008),

Pubmed(Namata et al., 2012), Citeseer(Sen et al., 2008), Amazon Photos(Shchur et al., 2018), Amazon Computers(Shchur et al., 2018), Coauthor CS(Shchur et al., 2018) and WikiCS(Mernyei & Cangea, 2020). Details on number of nodes, edges and features are given in table 1. Cora consists of 2708 scientific publications classified into one of seven classes, Citeseer consists of 3312 scientific publications classified into one of six classes and Pubmed consists of 19717 scientific publications pertaining to diabetes classified into one of three classes. In Amazon Photos and Amazon Computers, nodes represent goods and edges represent that two goods are frequently bought together. The product reviews are represented as bag-of-words features. Coauthor CS contains paper keywords for each author’s papers. Nodes represent authors that are connected by an edge if they co-authored a paper. WikiCS is a dataset derived from Wikipedia with nodes corresponding to Computer Science articles and edges based on hyperlinks. The 10 classes represent different branches of Computer Science.

Table 1: **Dataset Details**

Dataset	Nodes	Edges	Features	Classes
Cora	2,708	10,556	1,433	7
Citeseer	3,327	9,104	3,703	6
Pubmed	19,717	88,648	500	3
Amazon Photos	7,650	238,612	745	8
Amazon Computers	13,752	491,722	767	10
Coauthor CS	18,333	163,788	6,805	15
WikiCS	11,701	216,123	300	10

4.1.2 Evaluation Methodology

The embeddings are evaluated on node classification, whose performance is quantified by accuracy. We follow the same evaluation protocol as used in (Veličković et al., 2017), (Ding et al., 2023), (Ju et al., 2022) etc. All scores for baselines have been obtained from previously published papers.

4.1.3 Evaluation Protocol

For all downstream tests, we follow the linear evaluation protocol on graphs where the parameters of the backbone/encoder are frozen during inference time. Only the prediction head, which is a single GCN layer, is trained for node classification. For evaluation purposes, we use the default number for train/val/test splits for the citation networks i.e. Cora, Pubmed, Citeseer which are 500 validation and 1000 testing nodes. The train/val/test splits for the remaining datasets, namely, Amazon Photos, Amazon Computers and Coauthor CS are according to (Shchur et al., 2018). For WikiCS we use the publicly available splits. Unless otherwise mentioned, performance is averaged over 10 independent runs with different random seeds and splits for all seven evaluation datasets. We report the mean and standard deviation obtained across 10 runs.

4.1.4 Environment

To ensure a fair comparison, for all datasets, we use the same number of layers for the GNN encoder and the same number of features at each hidden layer. The encoder predicts 512 hidden features in the latent space for all datasets. The number of output features of the final classification head is the only parameter varied. We use a Cosine Annealing learning rate scheduler with warm restarts after 75 epochs, and early stopping is employed for all experiments.

4.2 Evaluation Results

4.2.1 Performance on Node Classification on small and large graphs

As mentioned earlier, we use the linear evaluation protocol and report the mean and standard deviation of classification accuracy on the test nodes over 10 runs on different folds or splits with different seeds. We

compare our proposed approach with supervised and fine-tuned model baselines. For semi-supervised node classification, we compare our proposed approach against Multi Layer Perceptron(MLP), Graph Convolution Network(GCN)(Kipf & Welling, 2016), Graph Attention Network(GAT)(Veličković et al., 2017), Simplified GCN(Wu et al., 2019), Logistic Regression and GraphSAGE(Hamilton et al., 2017). For GraphSAGE, we use the mean, maxpool and meanpool variants as described in (Shchur et al., 2018). We have compared our model’s performance against semi-supervised baselines in table 2. For self-supervised and fine-tuned node classification, we compare our proposed approach against DGI, MVGRL(Hassani & Khasahmadi, 2020), GRACE(Zhu et al., 2020), CCA-SSG(Zhang et al., 2021), SUGRL(Mo et al., 2022), S3-CL(Ding et al., 2023), GraphMAE(Hou et al., 2022), GMI(Peng et al., 2020), BGRL(Thakoor et al., 2021) and ParetoGNN(Ju et al., 2022) on small and large graphs. In semi-supervised node classification (Table 2), our method achieves the highest accuracy across all baselines. On self-supervised classification followed by fine-tuning, we evaluate our proposed model against two specific fields of data i.e Planetoid datasets and larger, more stable datasets such as Amazon Computers, Photos and WikiCS. Table 3 compares our model’s performance against strong baselines on Planetoid datasets. We show that our model performs extremely well on smaller datasets by outperforming all baselines on Cora and Citeseer with extremely competitive results on Pubmed. Table 4 contains the performance of our model against strong baselines for Photos, Computers, Coauthor CS and WikiCS. Our model consistently achieves competitive scores against baselines by outperforming baselines on Photos and CS while remaining competitive on Computers and WikiCS .These results underscore the approach’s adaptability and strong performance across diverse dataset sizes. Owing to the ability of our proposed approach to avoid noisy features, representation collapse, and leverage semantic information, our proposed model performs well on small and unstable datasets such as Cora and Citeseer and large datasets such as Amazon, Coauthor and WikiCS.

Table 2: **Semi-Supervised Node Classification.** The values indicate the accuracy achieved on node classification by several methods. A higher value indicates better performance. The best score is marked in **bold** and the second-best score is underlined. N/A indicates that the score was not reported for a particular dataset by the original authors.

Method	Cora	Citeseer	Pubmed	Photos	Computers	Coauthor CS
MLP	55.2 ± 0.4	46.5 ± 0.5	71.4 ± 0.3	78.5 ± 0.2	44.9 ± 5.8	76.5 ± 0.3
GCN	81.5 ± 1.3	71.9 ± 1.9	77.8 ± 2.9	91.2 ± 1.2	82.6 ± 2.4	91.1 ± 0.5
GAT	<u>81.8 ± 0.3</u>	71.4 ± 1.8	78.7 ± 2.3	85.7 ± 20.3	78.0 ± 19.0	90.5 ± 0.6
Simplified GCN	81.5 ± 0.2	73.1 ± 0.1	79.7 ± 0.4	88.3 ± 1.1	N/A	91.5 ± 0.3
GraphSage Mean	79.2 ± 7.7	71.6 ± 1.9	<u>77.4 ± 2.2</u>	<u>91.4 ± 1.3</u>	82.4 ± 1.8	<u>91.3 ± 2.8</u>
GraphSage MaxPool	76.6 ± 1.9	67.5 ± 2.3	76.1 ± 2.3	90.4 ± 1.3	N/A	85.0 ± 1.1
GraphSage MeanPool	77.9 ± 2.4	68.6 ± 2.4	76.5 ± 2.4	90.7 ± 1.6	79.9 ± 2.3	89.6 ± 0.9
Logistic Regression	57.1 ± 2.3	61.0 ± 2.2	64.1 ± 3.1	73.0 ± 6.5	64.1 ± 5.7	86.4 ± 0.9
Ours	89.8 ± 0.9	77.0 ± 0.9	85.7 ± 1.0	94.5 ± 0.5	88.0 ± 0.6	94.5 ± 0.4

4.2.2 Study on GMM Cluster Optimization

In this section, we evaluate the significance of the constraint in our loss function. Our approach combines learning sub-graph embeddings with optimizing node embeddings using pseudo-labels derived from a Gaussian Mixture Model (GMM). These pseudo-labels, converted to normalized scores, serve as a constraint in the original loss function for subgraph embeddings. Table 5 illustrates the performance of our method with and without this constraint, demonstrating a substantial improvement when the GMM-derived pseudo-label scores are incorporated. This finding is particularly noteworthy as it indicates that computationally expensive processes like negative sampling, commonly used in graph contrastive learning, may not be essential for optimizing node embeddings. Our approach thus offers a more efficient alternative while maintaining, and even enhancing, performance in graph representation learning tasks.

4.2.3 Study on Momentum Parameter m

Figure 2 represents the change in performance with respect to the momentum parameter on the citeseer dataset. The ideal values for m may range between 0.8 and 0.9. As $m \rightarrow 1$, the weights of the target

Table 3: **Self Supervised Pre-Training followed by classification on Planetoid Datasets.** The values indicate the accuracy achieved on node classification by several SSL methods. A higher value indicates better performance. The best score is marked in bold and the second-best score is underlined.

Method	Cora	Citeseer	Pubmed
DGI	81.7 ± 0.6	71.5 ± 0.7	77.3 ± 0.6
MVGRL	82.9 ± 0.7	72.6 ± 0.7	79.4 ± 0.3
GRACE	80.0 ± 0.4	71.7 ± 0.6	79.5 ± 1.1
CCA-SSG	84.2 ± 0.4	73.1 ± 0.3	81.6 ± 0.4
SUGRL	83.4 ± 0.5	73.0 ± 0.4	81.9 ± 0.3
S3-CL	<u>84.5 ± 0.4</u>	<u>74.6 ± 0.4</u>	80.8 ± 0.3
GraphMAE	84.2 ± 0.4	73.1 ± 0.4	83.9 ± 0.3
GMI	82.7 ± 0.2	73.3 ± 0.3	77.3 ± 0.6
BGRL	83.8 ± 1.6	72.3 ± 0.9	86.0 ± 0.3
Ours	89.8 ± 0.9	77.0 ± 0.9	<u>85.7 ± 1.0</u>

Table 4: **Self Supervised Pre-Training followed by classification on datasets mentioned in Shchur et al. (2018) and WikiCS.** The best score for each dataset is marked in bold and the second-best score is underlined.

Method	Photos	Computers	Coauthor CS	WikiCS
DGI	91.6 ± 0.2	83.9 ± 0.5	92.1 ± 0.6	75.3 ± 0.1
GRACE	92.1 ± 0.5	86.7 ± 0.8	93.2 ± 0.4	77.5 ± 0.6
BGRL	93.2 ± 0.3	<u>90.3 ± 0.2</u>	<u>93.3 ± 0.1</u>	80.0 ± 0.1
ParetoGNN	<u>93.8 ± 0.3</u>	90.7 ± 0.2	92.2 ± 0.1	82.9 ± 0.1
MVGRL	93.2 ± 0.3	87.5 ± 0.1	92.1 ± 0.1	77.5 ± 0.1
Random Weights	92.1 ± 0.5	86.5 ± 0.4	91.6 ± 0.3	78.9 ± 0.6
Ours	94.5 ± 0.5	88.0 ± 0.6	94.5 ± 0.4	<u>82.4 ± 1.0</u>

Table 5: **Ablation Study for Loss Function.** The best score for each dataset is marked in bold.

Method	Cora	Citeseer	Pubmed	Photos	Computers	Coauthor CS	WikiCS
Without Bayesian Inference	89.0	74.1	84.2	93.4	85.0	93.2	81.5
With Bayesian Inference	89.8	77.0	85.7	94.5	88.0	94.5	82.4

encoder update by very small steps, thereby slowing down learning. This is further indicated by the drop in performance. For all our experiments, we use $m = 0.9$.

4.2.4 Efficiency Analysis for Scalability

We evaluate the model’s efficiency in terms of the parameter size and memory consumption. We show that our model is among the most efficient of all baselines while outperforming most baselines. We compare the efficiency of our proposed model against reported baselines in table 6.

4.2.5 Study on Performance against Test Time Node Feature Distortion

We evaluate the performance of our method on node classification by augmenting the test splits. We sample p percentage test nodes randomly and replace their node features with points sampled from a standard Gaussian distribution. We evaluate the performance of the distorted test nodes on Amazon Computers,

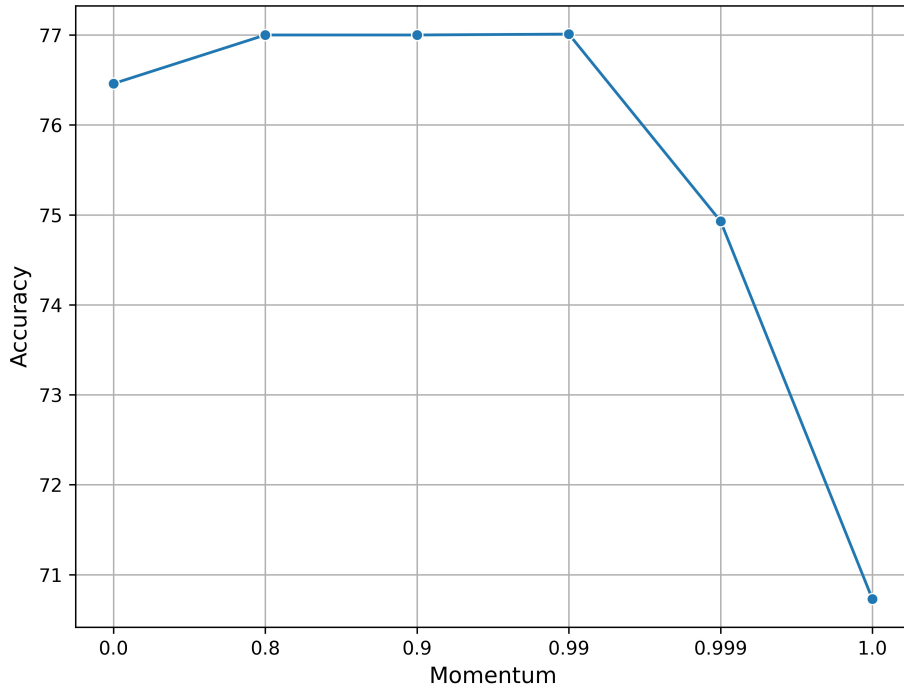


Figure 2: Variation of accuracy with respect to momentum parameter m on Citeseer

Table 6: **Efficiency Comparison among Baselines on Cora, Pubmed, and Citeseer.** Lower the number of parameters, more efficient is the model

Methods	Cora		Citeseer		Pubmed	
	Memory (GB)	Params	Memory (GB)	Params	Memory (GB)	Params
DGI	3.73	7.3×10^5	3.85	1.9×10^6	3.66	2.6×10^5
GMI	4.06	9.9×10^5	4.20	2.2×10^6	3.93	5.2×10^5
MVGRL	2.25	9.9×10^5	2.55	2.2×10^6	2.37	5.2×10^5
SUGRL	1.57	9.7×10^5	1.71	2.6×10^6	1.70	3.9×10^5
S ³ -CL	1.37	7.3×10^5	1.62	1.9×10^6	1.54	2.6×10^5
Ours	0.70	3.5×10^5	0.80	6.4×10^5	1.90	2.3×10^5

WikiCS, Amazon Photos and Coauthor CS by varying p between 10% and 40% and report their performance differences in table 7. In this study, we only use WikiCS, Co-author and Amazon networks since Planetoid datasets tend to be unstable on evaluation as indicated in (Shchur et al., 2018). Despite no further fine-tuning on distorted node features, the average performance drop on Amazon Photos and Computers is only 2.96% and 4.01% respectively. This indicates the ability of the joint framework to generalize on noise-augmented views as well. According to our hypothesis, we believe this is due to the nature of joint predictive embedding learning where a higher variation in context and target embeddings is required for better generalization.

Table 7: **Performance on distorting node features at test time.** Values represent the percentage decrease in the model’s performance compared to its original score. A lower value indicates better performance.

Ratio	Photos	Computers	Coauthor CS	WikiCS
0.10	-3.3%	-3.8%	-3.3%	-8.9%
0.15	-0.8%	-3.4%	-1.2%	-9.7%
0.20	-3.7%	-3.3%	-3.3%	-13.6%
0.25	-2.9%	-4.6%	-7.7%	-12.6%
0.30	-3.9%	-4.3%	-5.9%	-13.2%
0.35	-2.4%	-4.0%	-6.6%	-12.3%
0.40	-3.7%	-4.7%	-9.6%	-15.2%

5 Conclusion

In this paper, we propose a novel Graph Self-Supervised Learning (Graph-SSL) framework that combines joint predictive embedding and pseudo-labeling to effectively capture global knowledge while avoiding noisy features and bypassing contrastive methods such as negative sampling and reconstruction. The joint predictive embedding framework leverages the context-target relationship between node embeddings in the latent space by predicting multiple target embeddings for a single context. This approach, combined with the optimization of node feature contributions to pseudo-labels, enables a lightweight Graph Neural Network (GNN) encoder to capture intricate patterns in both graph structure and node features without requiring the stacking of multiple layers or encoders. Additionally, our method addresses the node representation collapse problem by incorporating information from multiple targets for a single context, ensuring robust and diverse embeddings. Through extensive experiments on multiple benchmark graph datasets, we demonstrate that our proposed framework achieves superior performance compared to several state-of-the-art graph self-supervised learning methods.

References

- Mahmoud Assran, Quentin Duval, Ishan Misra, Piotr Bojanowski, Pascal Vincent, Michael Rabbat, Yann LeCun, and Nicolas Ballas. Self-supervised learning from images with a joint-embedding predictive architecture. In *Proceedings of the IEEE/CVF Conference on Computer Vision and Pattern Recognition*, pp. 15619–15629, 2023.
- Kaize Ding, Yancheng Wang, Yingzhen Yang, and Huan Liu. Eliciting structural and semantic global knowledge in unsupervised graph contrastive learning. In *Proceedings of the AAAI Conference on Artificial Intelligence*, volume 37, pp. 7378–7386, 2023.
- Zhengcong Fei, Mingyuan Fan, and Junshi Huang. A-jepa: Joint-embedding predictive architecture can listen. *arXiv preprint arXiv:2311.15830*, 2023.
- Will Hamilton, Zhitao Ying, and Jure Leskovec. Inductive representation learning on large graphs. *Advances in neural information processing systems*, 30, 2017.
- Kaveh Hassani and Amir Hosein Khasahmadi. Contrastive multi-view representation learning on graphs. In *International conference on machine learning*, pp. 4116–4126. PMLR, 2020.
- Zhenyu Hou, Xiao Liu, Yukuo Cen, Yuxiao Dong, Hongxia Yang, Chunjie Wang, and Jie Tang. Graphmae: Self-supervised masked graph autoencoders. In *Proceedings of the 28th ACM SIGKDD Conference on Knowledge Discovery and Data Mining*, pp. 594–604, 2022.
- Ming Jin, Yizhen Zheng, Yuan-Fang Li, Chen Gong, Chuan Zhou, and Shirui Pan. Multi-scale contrastive siamese networks for self-supervised graph representation learning. *arXiv preprint arXiv:2105.05682*, 2021a.

-
- Wei Jin, Xiaorui Liu, Xiangyu Zhao, Yao Ma, Neil Shah, and Jiliang Tang. Automated self-supervised learning for graphs. *arXiv preprint arXiv:2106.05470*, 2021b.
- Mingxuan Ju, Tong Zhao, Qianlong Wen, Wenhao Yu, Neil Shah, Yanfang Ye, and Chuxu Zhang. Multi-task self-supervised graph neural networks enable stronger task generalization. *arXiv preprint arXiv:2210.02016*, 2022.
- Diederik P Kingma. Adam: A method for stochastic optimization. *arXiv preprint arXiv:1412.6980*, 2014.
- Thomas N Kipf and Max Welling. Semi-supervised classification with graph convolutional networks. *arXiv preprint arXiv:1609.02907*, 2016.
- Yuecheng Li, Jialong Chen, Chuan Chen, Lei Yang, and Zibin Zheng. Contrastive deep nonnegative matrix factorization for community detection. In *ICASSP 2024-2024 IEEE International Conference on Acoustics, Speech and Signal Processing (ICASSP)*, pp. 6725–6729. IEEE, 2024.
- Seiji Maekawa, Koki Noda, Yuya Sasaki, et al. Beyond real-world benchmark datasets: An empirical study of node classification with gnns. *Advances in Neural Information Processing Systems*, 35:5562–5574, 2022.
- Péter Mernyei and Cătălina Cangea. Wiki-cs: A wikipedia-based benchmark for graph neural networks. *arXiv preprint arXiv:2007.02901*, 2020.
- Yujie Mo, Liang Peng, Jie Xu, Xiaoshuang Shi, and Xiaofeng Zhu. Simple unsupervised graph representation learning. In *Proceedings of the AAAI conference on artificial intelligence*, volume 36, pp. 7797–7805, 2022.
- Galileo Namata, Ben London, Lise Getoor, Bert Huang, and U Edu. Query-driven active surveying for collective classification. In *10th international workshop on mining and learning with graphs*, volume 8, pp. 1, 2012.
- Zhen Peng, Wenbing Huang, Minnan Luo, Qinghua Zheng, Yu Rong, Tingyang Xu, and Junzhou Huang. Graph representation learning via graphical mutual information maximization. In *Proceedings of The Web Conference 2020*, pp. 259–270, 2020.
- Prithviraj Sen, Galileo Namata, Mustafa Bilgic, Lise Getoor, Brian Galligher, and Tina Eliassi-Rad. Collective classification in network data. *AI magazine*, 29(3):93–93, 2008.
- Oleksandr Shchur, Maximilian Mumme, Aleksandar Bojchevski, and Stephan Günnemann. Pitfalls of graph neural network evaluation. *arXiv preprint arXiv:1811.05868*, 2018.
- Shantanu Thakoor, Corentin Tallec, Mohammad Gheshlaghi Azar, Mehdi Azabou, Eva L Dyer, Remi Munos, Petar Veličković, and Michal Valko. Large-scale representation learning on graphs via bootstrapping. *arXiv preprint arXiv:2102.06514*, 2021.
- Petar Veličković, Guillem Cucurull, Arantxa Casanova, Adriana Romero, Pietro Lio, and Yoshua Bengio. Graph attention networks. *arXiv preprint arXiv:1710.10903*, 2017.
- Petar Veličković, William Fedus, William L Hamilton, Pietro Liò, Yoshua Bengio, and R Devon Hjelm. Deep graph infomax. *arXiv preprint arXiv:1809.10341*, 2018.
- Yuhu Wang, Jinyong Wen, Chunxia Zhang, and Shiming Xiang. Graph aggregating-repelling network: Do not trust all neighbors in heterophilic graphs. *Neural Networks*, 178:106484, 2024. ISSN 0893-6080. doi: <https://doi.org/10.1016/j.neunet.2024.106484>. URL <https://www.sciencedirect.com/science/article/pii/S0893608024004088>.
- Felix Wu, Amauri Souza, Tianyi Zhang, Christopher Fifty, Tao Yu, and Kilian Weinberger. Simplifying graph convolutional networks. In *International conference on machine learning*, pp. 6861–6871. PMLR, 2019.
- Zonghan Wu, Shirui Pan, Fengwen Chen, Guodong Long, Chengqi Zhang, and S Yu Philip. A comprehensive survey on graph neural networks. *IEEE transactions on neural networks and learning systems*, 32(1):4–24, 2020.

Hengrui Zhang, Qitian Wu, Junchi Yan, David Wipf, and Philip S Yu. From canonical correlation analysis to self-supervised graph neural networks. *Advances in Neural Information Processing Systems*, 34:76–89, 2021.

Muhan Zhang and Yixin Chen. Link prediction based on graph neural networks. *Advances in neural information processing systems*, 31, 2018.

Yanqiao Zhu, Yichen Xu, Feng Yu, Qiang Liu, Shu Wu, and Liang Wang. Deep graph contrastive representation learning. *arXiv preprint arXiv:2006.04131*, 2020.

A Declarations

A.1 Availability of Data and Materials

The datasets used in all experiments during this study are available in a publicly accessible repository. They can be obtained at <https://pytorch-geometric.readthedocs.io/en/latest/modules/datasets.html>

A.2 Code Availability

The codes used for all experiments in this study are designed by us and is available at <https://github.com/Deceptrax123/JPEB-GSSL>

A.3 Conflict of Interest

The authors declare that they have no conflicts of interest to report regarding the present study.